TISSUE ENGINEERING: Part C
Volume 20, Number 9, 2014

DOI: 10.1089/ten.tec.2013.0581

Methods to Analyze Bone Regenerative Response to Different rhBMP-2 Doses in Rabbit Craniofacial Defects

Teja Guda, PhD,[1,2,*] Aniq Darr, PhD,[3] David T. Silliman, BA,[1] Maria H.R. Magno, PhD,[3] Joseph C. Wenke, PhD,[4] Joachim Kohn, PhD,[3] and Pamela R. Brown Baer, MEd, DDS[1,*]

Multiple assessment methods are available to evaluate the performance of engineered scaffolds in accepted bone healing animal models. Evaluation and comparison of these methods can aid in the planning of future animal studies, as well as, inform clinical assessments as the engineered scaffolds translate into clinical studies and applications. To evaluate multiple bone assessment techniques, bone regrowth potential of tyrosine-derived polycarbonate (TyrPC) scaffolds loaded with various dosages of recombinant human bone morphogenetic protein-2 (rhBMP-2) (0, 10, 25, and 50 μg) was assessed after 16 weeks *in vivo* in a rabbit calvarial model. Traditional X-ray radiography and micro-computed tomography (micro-CT) analyses were used to quantify the volume and density of regenerated bone. Histomorphometric analysis was performed as the traditional gold standard of evaluation. While these techniques are fairly standard in bone tissue engineering, we also investigated 64-slice CT, a tool more commonly used clinically, for comparison and to guide translational efforts. The 64-slice CT scans were carried out at 4 and 16 weeks to monitor temporal bone healing patterns. Study results indicated a clear dose-dependent response of increasing regenerated bone volume with rhBMP-2 loaded on the TyrPC scaffolds after 16 weeks of implantation. Significantly more bone formation was observed at the highest dose of rhBMP-2 (50 μg), which is 25–50% of the previously recommended dose (100–200 μg) for this defect. A significant difference was observed between the lowest and highest doses using radiographs ($p < 0.001$), micro-CT (p 0.002), and CT ($p < 0.001$) and a high correlation was found between techniques (R^2 values between 0.446 and 0.911). It was found that the number of animals required per group to detect significant dose effects ranged between 6 and 8 for the imaging methods while histomorphometric analysis would require 25 animals per group to detect similar differences (desired power 0.9, α 0.05). Radiographic analysis provided quantifiable % defect coverage and radio-opacity, micro-CT provided spatial volumetric and bone density measures, histomorphometry provided biological confirmation, and 64-slice CT allowed for establishing of clinically relevant translational guidelines. These methodologies allow for a standardized and comprehensive description of bone regeneration and provide guidelines for the planning of future preclinical and clinical studies.

Introduction

The initial screening of synthetic grafts for tissue engineering occurs in animal models with the objective of further translation into clinical applications. During initial preclinical evaluation, it is critical to understand and maximize the advances in quantification methodologies available to evaluate and analyze the nature, quantity, and quality of bone regeneration. It is equally essential to compare and contrast the benefits and drawbacks of each of these analysis techniques with an eye on future clinical applicability. Previously, Hedberg *et al.*[1] compared the use of radiography, micro-computed tomography (micro-CT), and histology in a semiquantitative manner to evaluate bone regeneration in a

The work was performed primarily at the United States Army Institute of Surgical Research, Fort Sam Houston and at Rutgers, The State University of New Jersey.
[1]Department of Craniomaxillofacial Regenerative Medicine, Dental and Trauma Research Detachment, United States Army Institute of Surgical Research, Fort Sam Houston, Texas.
[2]Department of Biomedical Engineering, University of Texas at San Antonio, San Antonio, Texas.
[3]Department of Chemistry and Chemical Biology and New Jersey Center for Biomaterials, Rutgers, The State University of New Jersey, Piscataway, New Jersey.
[4]Department of Extremity Trauma and Regenerative Medicine, United States Army Institute of Surgical Research, Fort Sam Houston, Texas.
*These authors contributed equally to the preparation of this article.

Report Documentation Page

Form Approved
OMB No. 0704-0188

1. REPORT DATE	2. REPORT TYPE	3. DATES COVERED
01 SEP 2014	**N/A**	**-**

4. TITLE AND SUBTITLE	5a. CONTRACT NUMBER
Methods to analyze bone regenerative response to different rhBMP-2 doses in rabbit craniofacial defects.	5b. GRANT NUMBER
	5c. PROGRAM ELEMENT NUMBER
6. AUTHOR(S)	5d. PROJECT NUMBER
Guda T., Darr A., Silliman D. T., Magno M. H., Wenke J. C., Kohn J., Brown Baer P. R.,	5e. TASK NUMBER
	5f. WORK UNIT NUMBER
7. PERFORMING ORGANIZATION NAME(S) AND ADDRESS(ES)	8. PERFORMING ORGANIZATION REPORT NUMBER
United States Army Institute of Surgical Research, JBSA Fort Sam Hosuton, TX	
9. SPONSORING/MONITORING AGENCY NAME(S) AND ADDRESS(ES)	10. SPONSOR/MONITOR'S ACRONYM(S)
	11. SPONSOR/MONITOR'S REPORT NUMBER(S)

12. DISTRIBUTION/AVAILABILITY STATEMENT
Approved for public release, distribution unlimited

13. SUPPLEMENTARY NOTES

14. ABSTRACT

15. SUBJECT TERMS

16. SECURITY CLASSIFICATION OF:			17. LIMITATION OF ABSTRACT	18. NUMBER OF PAGES	19a. NAME OF RESPONSIBLE PERSON
a. REPORT	b. ABSTRACT	c. THIS PAGE			
unclassified	**unclassified**	**unclassified**	**UU**	**12**	

rabbit extremity model. In the current study, we compare and correlate fully quantitative methodologies for the same techniques and add 64-slice CT to analyze bone regeneration in a critical-size defect in a craniomaxillofacial model in rabbits.

Craniofacial bone grafts are in increasing demand to treat conditions ranging from bone augmentation prior to implant placement, fracture repair, healing large defects stemming from traumatic injuries, cancer resections, or congenital deformities.[2] The development of synthetic bone graft substitutes has evolved from the use of osteoconductive scaffold materials alone, to pairing them with suitable osteoinductive growth factors to either stimulate preseeded osteogenic cells or to recruit osteoprogenitors from the surrounding tissue. Bone morphogenetic protein-2 (BMP-2) has been one of the more widely studied growth factors for craniofacial bone defect healing.[3–5] This trend stems from the U.S. Food and Drug Administration's (FDA) initial approval to treat spinal and open traumatic fractures and followed by approval for use in the oral and maxillofacial realm in 2007 for sinus augmentations and localized alveolar ridge augmentations of defects associated with extraction sockets.[6] The commercially available INFUSE system (Medtronic Spinal and Biologics, Memphis, TN), comprising an absorbable collagen sponge plus recombinant human BMP-2 (rhBMP-2), has been considered a synthetic alternative to the long-standing gold standard of autologous bone grafting, but uses supraphysiological doses of the protein. These high doses result in a high cost of therapy and potentially multiple adverse effects in clinical use, including reported cervical swelling,[7] osteoclast activation resulting in transient bone resorption and cyst-like bone void formation,[8] as well as observations of heterotopic bone formation.[9] In an effort to reduce the quantity of rhBMP-2 required, while maintaining efficacy of fracture healing and defect closure, novel biomaterial strategies have focused on controlled delivery from scaffold materials to promote bone regeneration.[10,11]

The critical-sized rabbit calvarial defect model[12] has been widely used as a small animal model to evaluate bone void fillers. Additionally, it is an accepted safety and efficacy benchmark in the translational development of new graft materials.[13] As novel synthetic graft substitutes evolve from materials alone to carriers with bioactive growth factors, the analysis of bone healing must also change to obtain the maximum relevant information. This is all the more critical since *in vivo* studies are more time consuming and expensive, and the number of animals used are limited by ethical considerations.[1] Further, histological analysis and mechanical testing are inherently destructive and limit simultaneous application on a single sample. Within these constraints, it is essential that the most comprehensive analysis of the animal model be carried out to evaluate bone healing architecture, quantity, quality, and biology as well as biomaterial performance. This would serve to address the short-term goal of screening materials to identify optimal composition based on spatiotemporal bone healing response, as well as optimize performance assessment in future large animal model research and human clinical trials if a material meets the requisite demands.

While multiple groups have tested a variety of grafts in the rabbit calvarial model,[14–20] few have used multiple characterization techniques to evaluate *in vivo* regeneration in a fully quantitative fashion. In the current study, we used porous tyrosine-derived polycarbonate (TyrPC) scaffolds [nomenclature E1001(1k) in a library of polymers] with a calcium phosphate (CP) coating as our primary graft material. These scaffolds have been well characterized[21] and shown to be highly osteoconductive materials[22] that are also suitable for controlled sustained release of growth factors such as rhBMP-2.[23] While low doses of rhBMP-2 (50 μg) loaded on these scaffolds have been shown to elicit a robust bone healing response after 6 weeks in the rabbit calvaria,[23] a dose response to determine the minimal quantity of rhBMP-2 required has not been evaluated. In the current study, we assessed bone regeneration as a response to increasing doses of rhBMP-2 (0, 10, 25, or 50 μg) delivered in a critical-sized calvarial defect in rabbits over an extended 16-week implantation period. Bone regeneration was comprehensively studied using four evaluation techniques: (1) radiography to evaluate defect closure, (2) 64-slice CT to assess the temporal sequence of healing, (3) micro-CT for three-dimensional (3D) volumetric analysis, and (4) nondecalcified histomorphometry to serve both as confirmation of healing as well as to investigate the biological response to the scaffold material. Since bone volume within the defect was a common parameter quantified in all techniques, our study also allowed for a direct comparison of the results obtained from each of the methods used and highlighted the benefits of their simultaneous application. Additionally, while micro-CT can be performed sequentially over a time course on the same animal, in the case of small-animal rodent models,[24] it is far more involved to do the same for rabbits and larger animals, especially in non-extremity models. Thus, including the use of 64-slice CT, which is easily available in most trauma centers, allows not only correlation to the techniques used in preclinical models and destructive techniques such as histology, but also facilitates clinical translation as synthetic graft therapies mature.

The aim of this study is to use an accepted craniofacial animal model to evaluate a known material delivering multiple doses of rhBMP-2 and to employ multiple evaluative methodologies that allow for a standardized and comprehensive description of bone regeneration with clinical translational implications. This design allows us to compare, correlate, and highlight advantages and disadvantages of each technique.

Materials and Methods

Scaffold fabrication

In this study, E1001(1k), an inherently osteoconductive polymer composition chosen from the library of TyrPCs, was used to create porous scaffolds.[21] E1001(1k) is the notation chosen to denote the block copolymer desaminotyrosyl-tyrosine ethyl ester-*co*-10%-desaminotyrosyl-tyrosine-*co*-01%-poly(ethylene glycol)$_{1k}$ carbonate within the polymer library. E1001(1k) scaffolds were fabricated into 3D porous scaffolds as described previously[23] by a combination of solvent casting, porogen leaching, and phase-separation techniques. Briefly, scaffold coating was performed by first immersing the preformed scaffolds in an aqueous 1 M $CaCl_2$ solution under vacuum followed by freeze-drying for 4 h and successive precipitation of CP by

addition of 0.96 M K_2HPO_4 trihydrate (chemicals purchased from Sigma-Aldrich, St. Louis, MO). The scaffolds then underwent a final freeze-drying step for 24 h and were then air-dried overnight and sterilized using ethylene oxide (EtO) (AN74i; Andersen Products, Haw River, NC) prior to rhBMP-2 loading. Sterility was verified using a Steritest® colorimetric biological sterility indicator strip (AN-80; Andersen Products) which was packaged with the scaffolds. Under sterile conditions, the scaffolds were conditioned for 1 h with PBS to reduce hydrophobicity. The rhBMP-2 (Wyeth, Cambridge, MA) was dissolved in deionized water and different doses by group were added drop-wise to each scaffold (0, 10, 25, or 50 μg/scaffold). The final scaffolds were 15.2 mm (diameter) × 2.5 mm (thickness) to conform to the rabbit calvarial defect.

Animal surgery

This study was conducted in compliance with the Animal Welfare Act, the implementing Animal Welfare Regulations, and the principles of the Guide for the Care and Use of Laboratory Animals. Skeletally mature New Zealand White female rabbits (weighing 3.5 4.5 kg) were survived for 16 weeks to evaluate four groups treated with E1001(1k) scaffolds loaded with four different doses of rhBMP-2. Prior to anesthetic induction, a preemptive analgesic (buprenorphine hydrochloride 0.025 0.05 mg/kg) was administered. Anesthetization was accomplished by administration of 50 mg of Telazol followed by isoflurane (1 3%) delivered in 100% oxygen via a laryngeal mask airway. Following intubation, rabbits were placed sternally and the calvaria were prepared for aseptic surgery with Betadine scrub and alcohol rinse. A coronal incision was made and the soft tissues were reflected to expose the calvarium. Using a MicroAire (Charlottesville, VA) surgical hand piece with a trephine (Special Designs, La Vernia, TX) while irrigating with copious physiological saline, a single craniotomy (15 mm diameter) was prepared in the parietal bones centered across the mid-sagittal suture, posterior to the transverse suture. Care was taken to avoid dural tears. E1001(1k) scaffolds loaded with various dosages of rhBMP-2 (0, 10, 25, and 50 μg, $n = 10$/dose, 40 rabbits total) were placed into the craniotomies and soft tissues were approximated and sutured closed in layers. Prior to the conclusion of the surgery, a 25 μg/h transdermal fentanyl patch was affixed to the dorsum in the interscapular region after the hair was clipped and subcutaneous fluids (lactated ringer's solution or 0.9% NaCl, 50 mL) were administered. The 64-slice CT scans (Aquilion 64 Multislice Helical CT Scanner; Toshiba American Medical, Tustin, CA) were performed at 4 and 16 weeks under anesthesia to evaluate bone regeneration within the craniotomies. Animals were survived for 16 weeks at which they were euthanized humanely using 1.0 mL of Fatal Plus via a femoral IV injection after anesthesia induction. Posteuthanasia, the calvarial bones were excised, radiographed, and placed in 10% formalin solution for fixation prior to micro-CT and histological evaluations. Two samples from the 10 μg rhBMP-2 dose group were not appropriately processed (8 remained) during evaluation and the 64-slice CT data and histomorphometry and successive correlation analysis only included a total of 38 samples (10 samples from each of the other three groups).

Radiographic analysis

Radiographs were acquired using a Faxitron MX20 X-ray Digital System (Faxitron X-ray Corporation, Wheeling, IL) for each calvarium after extraction. The images were captured at 25 kV at a 15 s exposure time and imported into the Faxitron DR Software (v3.2.2). For quantification, the images were exported as bitmap files using window levels 1396/184. CTAn software v1.11 (Skyscan, Kontich, Belgium) was used to analyze the % defect area coverage and relative X-ray attenuation through the defect thickness for each treatment group. A 15 mm region identical to the size of the defect created during the original study was outlined on each X-ray and automated thresholding was performed within this region using the Otsu method[25] across all samples to determine the mineralized tissue within the defect. The percent of the defect area filled by the mineralized tissue was measured as a ratio of the pixels of gray above the threshold to the total number of pixels in the defect area. The relative X-ray attenuation through the defect was determined as the ratio of the mean grayscale level of the mineralized tissue within the defect to the mean grayscale value of the mineralized tissue of the surrounding host bone.[26]

64-Slice CT analysis

64-Slice CT scan images were acquired at 4 and 16 weeks. These images had an effective pixel size of 500 μm. Three-dimensional rendering of the image sets was performed using a standard ''bone mask'' in Vitrea Core (v.6.3.2089.106; ViTAL, Minnetonka, MN). They were then coregistered for both the clinical time-points with the micro-CT for each corresponding sample at 16 weeks. The clinical volumes were then upsampled using trilinear interpolation by a factor of 25, so that the resolutions were in a similar range to the CT scans (20 μm). The image stack was then imported into Microview (GE Healthcare, Piscataway, NJ) and a region of interest (ROI) of 15 mm in diameter and 3.5 mm in depth was created to cover the defect site. A threshold of 428 mgHA/cc was selected across all samples using the Otsu algorithm[25] to distinguish mineralized tissue from unmineralized tissue within the defect. The bone volume fraction and bone mineral density of the mineralized tissue were calculated within the ROI for each sample.

Micro-CT analysis

Micro-CT analysis was performed using the Skyscan 1072 scanner (Bruker-MicroCT, Kontich, Belgium) at a resolution of 11.44 μm pixel while samples were hydrated with formalin. The images were reconstructed using NRecon software (Bruker-MicroCT) to generate grayscale images ranging from 0 to 255. DataViewer was used to realign the calvarial images so that the primary axes were the principal axes of the cylindrical defect space. Samples were then thresholded globally using the Otsu algorithm across all the groups in the study. The 15 mm defect created was then located to define the ROI. This region was 3.5 mm thick and its thickness was centered to account for the native curvature of the calvarium. Three-dimensional volume (bone volume to total volume ratio), bone mineral density, and morphometric analysis were carried out on CT images using CTanalyzer. Bone mineral

density of the regenerated bone tissue was normalized to the mineral density of the native calvarial bone for comparison with other techniques. To determine trabecular bone organization, histomorphometric parameters were computed for each of the scaffolds over the entire 3D volume to evaluate ossification connectivity. The parameters computed were trabecular pattern factor (Tb.Pf) and structural model index (SMI). Three-dimensional-volume models of the scaffolds were generated from the micro-CT scans using Mimics (v13.0; Materialise, Leuven, Belgium) for visualization.

Histological analysis

The excised calvarial implants were prepared for histology as previously described.[23] Briefly, samples were dehydrated in ascending grades of ethanol, followed by xylene at 4°C and then embedded in poly(methyl methacrylate). The specimens were then cut and ground to 30 μm thick sections using a diamond saw and MicroGrinder (Exakt Technologies, Oklahoma City, OK). The sections were mounted on slides and stained with Sanderson's Rapid Bone Stain and counterstained with van Gieson's picrofuchsin, to stain soft tissue blue and stain bone pink/red.

Complete histology slide images were acquired at 2.5× magnification on an Olympus SZX16 Research High-Class Stereo Microscope (Olympus Corp., Center Valley, PA) with an Olympus PD71 Microscope Digital Camera and compiled using the Olympus DP Manager software 3.2.1.276. Images were then loaded into Photoshop (v7.0.1; Adobe Systems, Inc., San Jose, CA). The entire defect area was selected within the ROI by manually tracing the outer boundary and the number of pixels was quantified. Within the defined defect area, the mineralized tissue was selected by color threshold of the pink/red stain and the number of bone pixels was measured. The percent mineralized tissue was calculated as the ratio of the mineralized tissue to the defect area.

Statistical analysis

All data are represented as mean ± standard error of the mean. Significance in radiographic, CT, micro-CT, and histological measures reported was determined using a one-way ANOVA and Tukey's test for *post hoc* evaluation when significance was found. In the case of Tb.Pf, SMI, and bone surface to bone volume ratio calculated from 3D micro-CT datasets, the normality test was met, but the equal variance test was not satisfied. These groups were consequently analyzed using the Kruskal Wallis test with Tukey's test for *post hoc* analysis. Significance level was set at $p < 0.05$ for all statistical measures reported. The different analysis methods used to quantify bone volume regenerated were standardized by Fisher's Z transformation and then correlated using Pearson's product moment correlation statistics (SigmaPlot v11.0; Systat Software, Inc., San Jose, CA) to determine confidence intervals and to find significant correlations. To determine the relative efficacy of techniques, the results from the analyses were used to calculate the minimum detectable difference between the means of the lowest and highest dose of rhBMP-2 used, 10 and 50 μg, and the standard deviation of residuals for each technique. Based

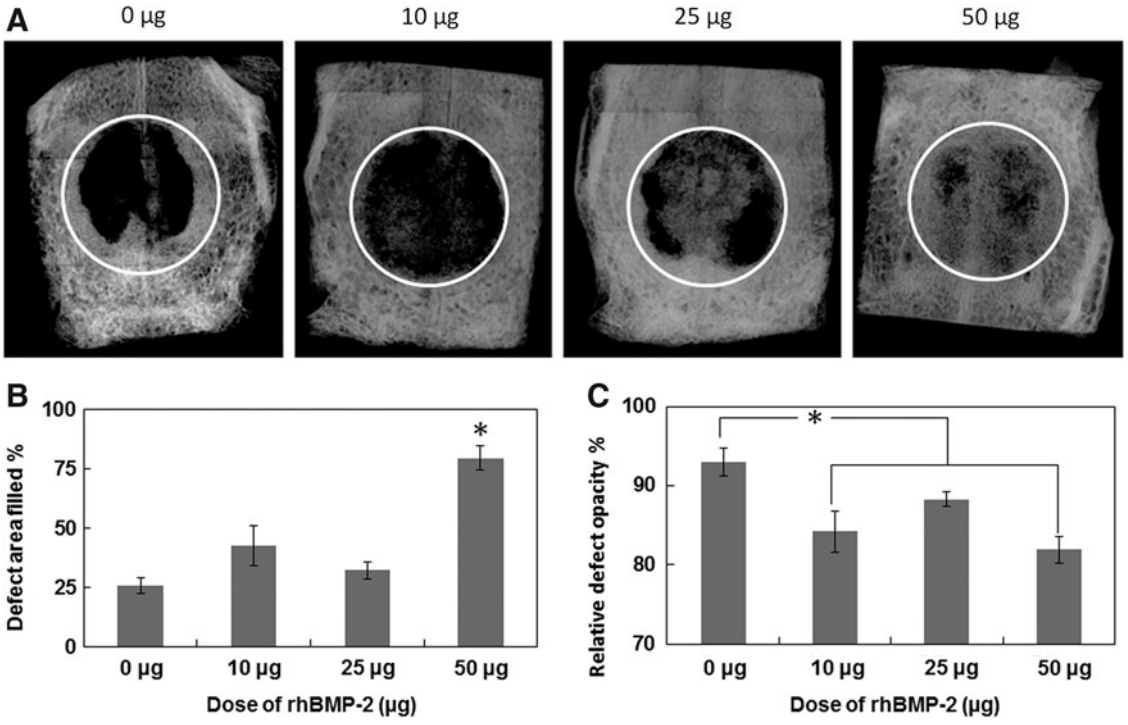

FIG. 1. Radiographic analysis of bone regeneration showing **(A)** representative image of a sample at each recombinant human bone morphogenetic protein-2 (rhBMP-2) dose and quantification of **(B)** defect area coverage by regenerated bone and **(C)** percentage opacity of the defect normalized to surrounding calvarial opacity after 16 weeks *in vivo*. Significant differences with $p < 0.01$ indicated by (*). Circles define defect area.

on these results, the suggested sample size for each technique was calculated to run ANOVA across four groups with a desired power = 0.9 and $\alpha = 0.05$.

Results

Radiographic analysis

Representative radiographs from each group are shown in Figure 1A. Radiographic analysis of the calvarial samples immediately posteuthanasia revealed differing levels of defect coverage, with the 50 μg rhBMP-2 dose showing almost twice as much defect area coverage (79% ± 5%) as the 10 and 25 μg doses (42% ± 8% and 32% ± 4%, respectively). The control group with no rhBMP-2 showed the least area coverage at 26% ± 3% (Fig. 1B). When the relative opacity of the pixels in the defect area was normalized to that of the pixels in the surrounding calvaria, it was observed that the regenerated mineralized tissue within the defect showed highest density in the control 0-μg rhBMP-2 group. The groups with 10 and 50 μg doses were significantly less dense than the control group ($p < 0.01$) (Fig. 1C). Since radiographic density is additive over a thick sample, this evaluation offered a perspective on the regenerative trends across groups through a parameter that combined regenerated mineral density with the distribution of bone along the depth of the calvarial defect.

64-Slice CT analysis

Cranial scans of the rabbits were performed at 4 and 16 weeks and the reconstructed images were viewed on the clinical CT visualization software. Representative images of the same animal at 4 and 16 weeks are shown in Figure 2A and clearly demonstrate that all groups increased in volume regenerated from the early to the late time point. The bone volume to tissue volume ratio quantification across all samples also indicated that all groups increased from 4 to 16 weeks ($p < 0.005$). From the 4 week data, it was observed that the bone volume fraction in the 50 μg dose group was significantly higher than at the 10 μg dose ($p < 0.02$) with neither of the other groups showing significant differences. At 16 weeks, the 25 μg dose regenerated significantly higher bone volume fraction than the control and 10 μg doses ($p < 0.01$) and the 50 μg dose at 76.5% ± 2.3% was significantly higher than all other doses ($p < 0.05$) of rhBMP-2 evaluated (Fig. 2B). The same differences between groups were also observed for the regenerated bone mineral density. While all groups had similar mineral density at 4 weeks

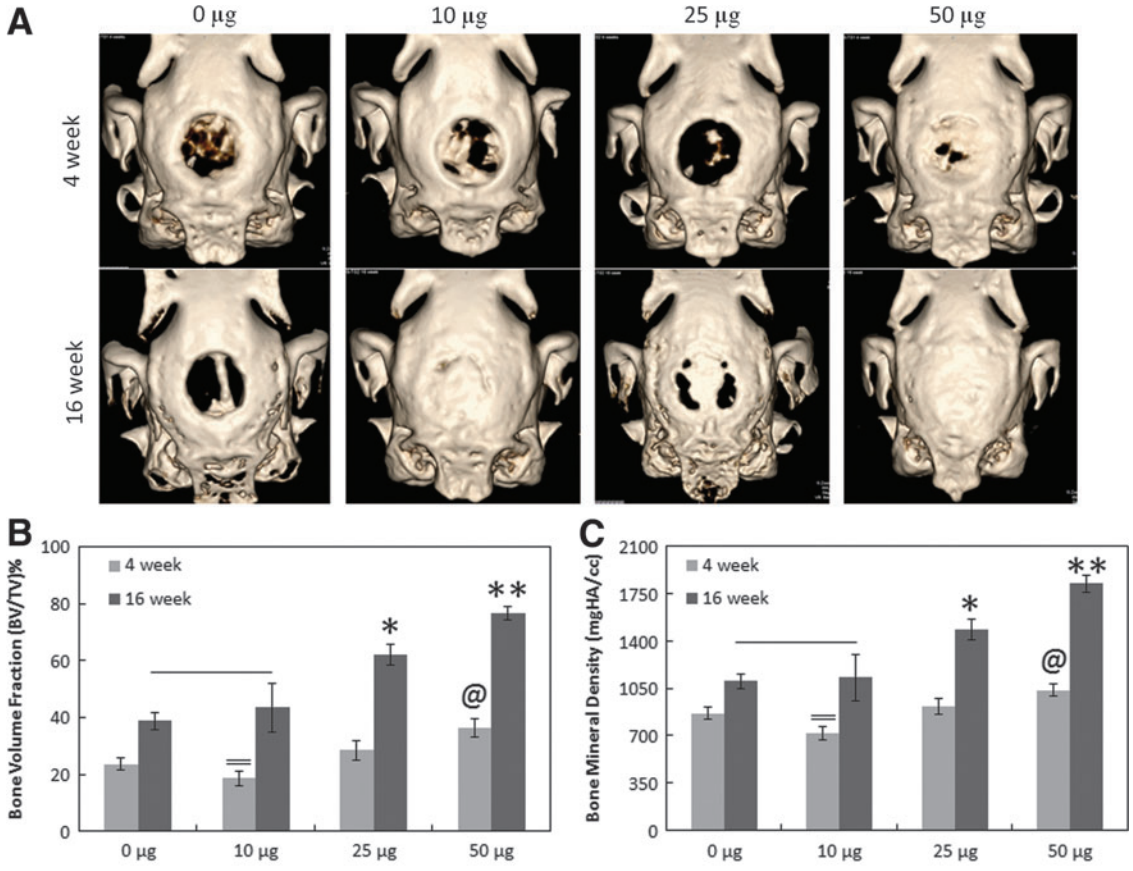

FIG. 2. **(A)** 64-Slice CT images acquired from the same animal at both 4 and 16 weeks for each rhBMP-2 dose are shown. **(B)** Bone volume regenerated within the defect and **(C)** bone mineral density of the regenerated bone are shown after 4 and 16 weeks *in vivo*. The bone volume regenerated and mineral density within the defect significantly increased from 4 to 16 weeks across all groups ($p < 0.001$). Significant differences ($p < 0.05$) were found between 10 and 50 μg doses at 4 weeks (indicated by = differing from @), and within the groups at 16 weeks; groups indicated by (*, **) are significantly different ($p < 0.05$) from all other doses not similarly labeled. Color images available online at www.liebertpub.com/tec

(average: 884 mg/cc, range: 718 1035 mg/cc among groups), there was a significant increase within each group from 4 to 16 weeks ($p < 0.05$). At 16 weeks, the 25 μg dose regenerated significantly higher bone mineral density than the control and 10 μg doses ($p < 0.01$) and the 50 μg dose at 1820 ± 66 mg/cc was significantly higher than all other doses of rhBMP-2 evaluated (Fig. 2C).

Micro-CT analysis

Micro-CT analysis of the excised calvaria after 16 weeks of implantation showed a clear dose effect of rhBMP-2 on the bone volume regenerated. Representative 3D reconstruction of the sample from each group that showed bone volume/tissue volume ratio closest to the group mean is shown in Figure 3A. These individual samples were also chosen to represent results from other techniques in Figures 1, 2, and 4. The bone volume to tissue volume ratio within the ROI was significantly higher in the 50 μg dose group when compared with the control and 10 μg dose ($p < 0.005$, Fig. 3B). The relative bone mineral density at the 50 μg dose was also significantly greater than the 10 μg dose ($p < 0.005$, Fig. 3C).

Spatial 3D morphometric analysis of the regenerated bone also allowed quantification of advanced parameters that indicate connectivity (trabecular number) and trabecular-like architecture (Tb.Pf) of the regenerated tissue (Fig. 3D, E). It was observed that the trabecular number was significantly higher at the 50 μg dose than at the 0 or 10 μg dose, while the Tb.Pf was significantly lower at the 50 μg dose than at the 0 or 10 μg dose. An evaluation of the depth

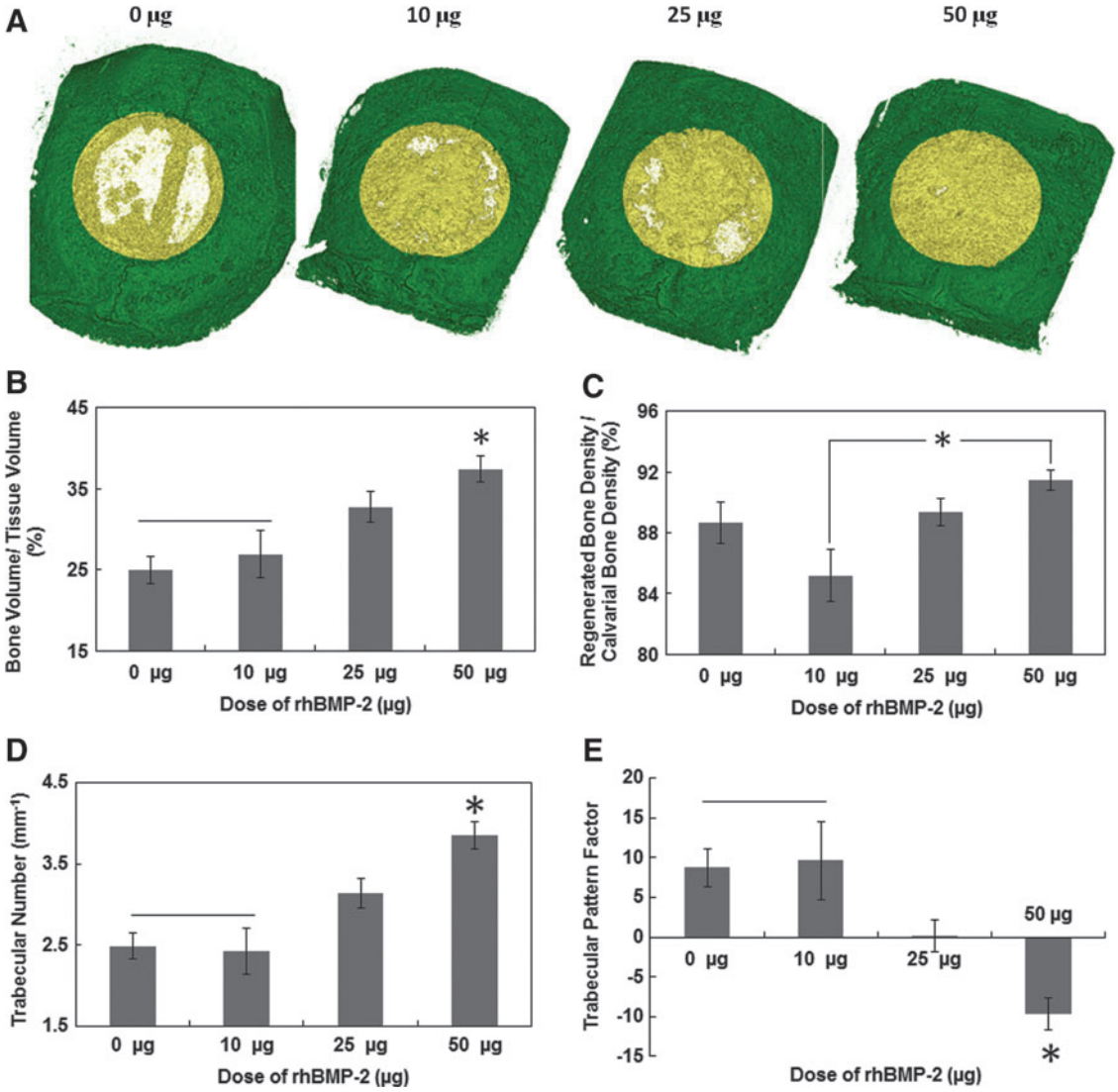

FIG. 3. **(A)** Representative samples at each rhBMP-2 dose were rendered in 3D from the micro-computed tomography (micro-CT) data and the new bone regenerated in the defect, shown within the circle, is contrasted with the surrounding native bone. Dose response was evaluated in 3D across **(B)** bone volume to tissue volume ratio where the 50 μg dose performed significantly better than the 0 and 10 μg doses ($p < 0.005$) and **(C)** bone mineral density normalized to calvarial density where the 50 μg dose performed significantly better than the 10 μg dose alone ($p < 0.005$) as indicated by (*). Advanced 3D morphometric analysis of the micro-CT data across showed that both **(D)** trabecular number and **(E)** trabecular pattern factor indicated that regenerated bone connectivity was significantly higher at the 50 μg dose than the 0 and 10 μg doses ($p < 0.05$) as indicated by (*). Color images available online at www.liebertpub.com/tec

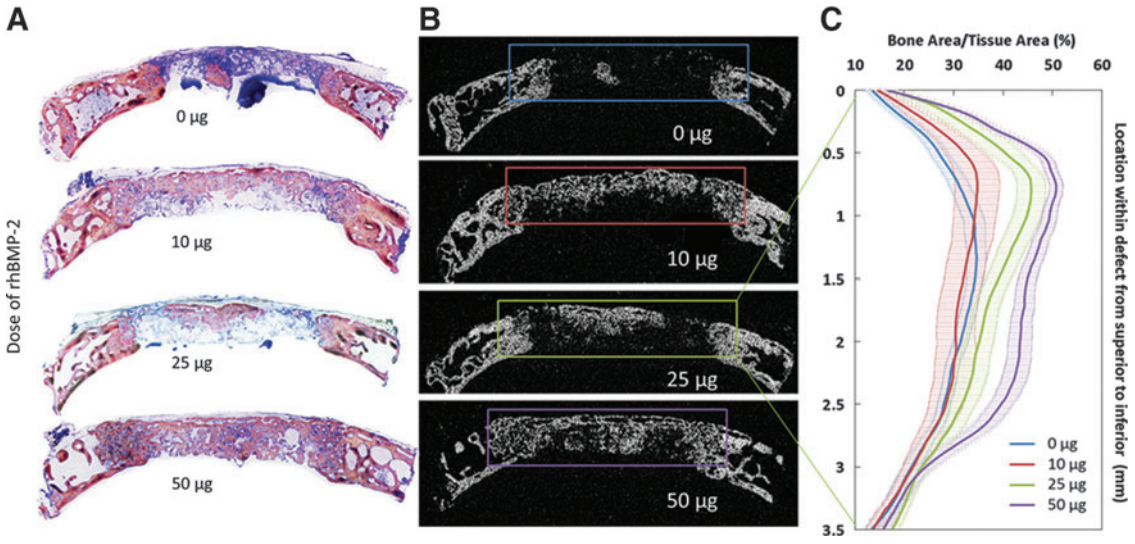

FIG. 4. Representative **(A)** histological images (1.5×) and corresponding **(B)** micro-CT coronal sections from the same animal are shown to indicate bone healing response at each dose after 16 weeks of implantation. Histological sections were stained with Sanderson's Rapid Bone stain and counterstained with van Gieson's picrofuchsin resulting in soft tissue staining blue and bone staining pink/red. Colored rectangles highlight the defect area. **(C)** A representation of the regenerated bone area fraction per slice from the superior to the inferior aspect of the defect from the micro-CT analysis, showed significant differences with dose on the spatial patterns of bone regeneration.

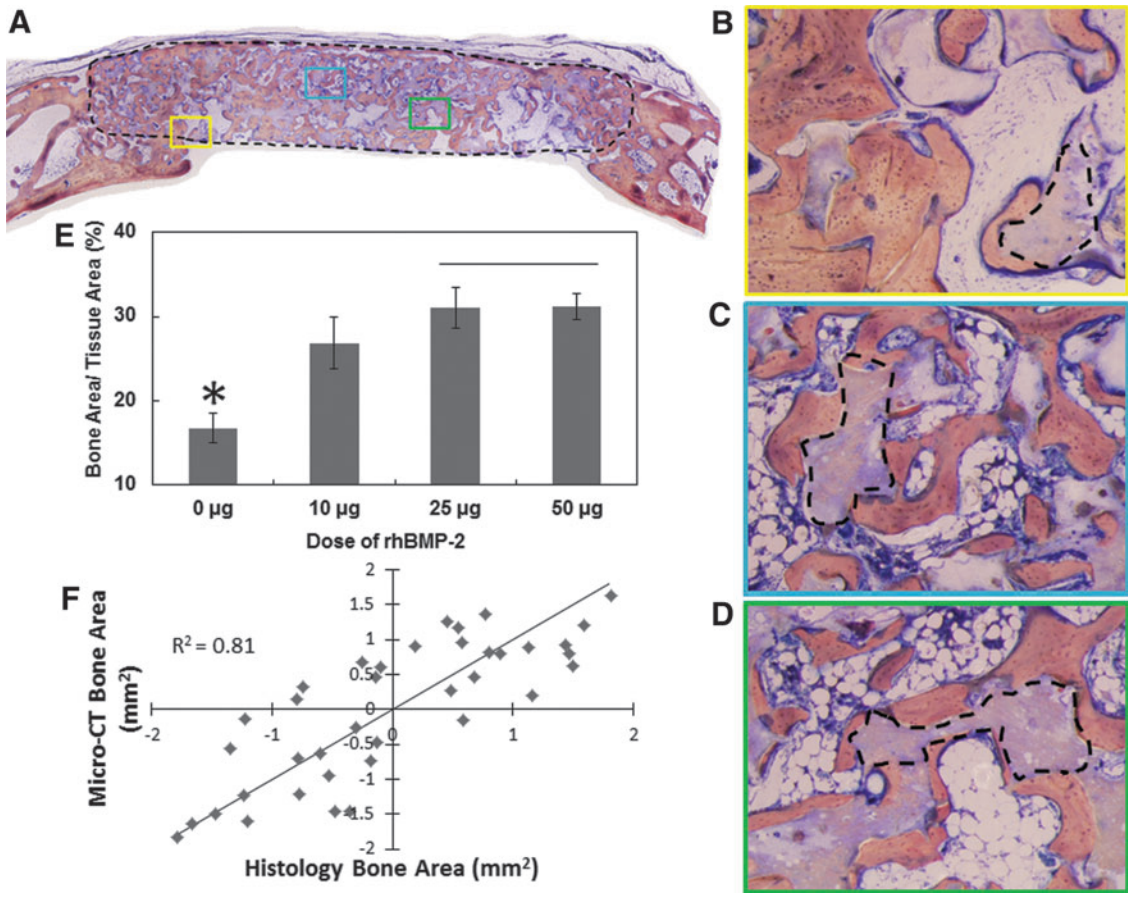

FIG. 5. **(A)** Histological image of a sample from the 50 µg rhBMP-2 dose group is shown at 1.5× magnification with rectangles highlighting insets at different radial locations **(B–D)** shown at 5× magnification to indicate bone formation in a trabecular-like pattern immediately adjacent to the scaffold/locations of scaffold resorption (black-dotted outlines) and an overall lack of local inflammatory response after 16 weeks. **(E)** A significantly lower bone area fraction ($p < 0.001$) was observed without rhBMP-2 compared with the 25 and 50 µg groups with rhBMP-2 (indicated by *). **(F)** A high correlation ($R^2 = 0.81$) was observed between the two-dimensional histology and corresponding micro-CT slices (data shown have been transformed by Fisher's Z transformation).

profile of the regenerated bone within the 3.5 mm thick defect ROI reveals that there is a bias in terms of greater coverage and regeneration in the superior aspect of the defect compared with the inferior aspect (Fig. 4). This trend was most conspicuous at the 25 μg dose, while there was greater uniformity across the defect depth at other doses of rhBMP-2 (Fig. 4C). Additionally, the 50 μg dose was observed to consistently regenerate greater bone at every depth within the defect compared with the other three groups.

Histological analysis

High correlation between the two-dimensional (2D) histological sections and 3D micro-CT-based datasets was observed ($R^2 = 0.656$), with corresponding matching images from the two techniques shown in Figure 4. Histomorphometry-based evaluation of bone area to tissue area ratio within the slides (Fig. 5) indicated that the bone area fraction was significantly lower in the group without rhBMP-2 compared with the 25 and 50 μg rhBMP-2-loaded groups ($p < 0.001$, Fig. 5E). An increase in bone area fraction regenerated was observed in the histological sections of the groups with 25 and 50 μg doses compared with the 10 μg dose, but this trend was not statistically significant ($p = 0.13$). The correlation between the histomorphometric bone area regenerated and an analysis of the corresponding 2D micro-CT slices was also excellent ($R^2 = 0.81$), validating the methods used in each case (Fig. 5F). Higher magnification qualitative evaluation (Fig. 5B D) of the histological slides indicated healthy bone tissue distributed throughout the defect space to varying extents depending on the rhBMP-2 dose. The regenerated bone (stained pink/red) was seen to grow immediately adjacent to the scaffold with no intermediate fibrous tissue or evident signs of inflammation. Scaffold degradation was also evident within the samples (clear regions within the outlined black borders of the scaffold in some locations). Clearly visible osteocytes, osteoblasts, blood vessels (at higher magnifications, data not shown), and mineralizing collagenous osteoid as well as mature bone were found in the defect interior, indicating a stable balance in the induced bone regeneration.

Comparison between analysis techniques

A clear dose-based response of increasing regenerated bone volume with rhBMP-2 loaded on the graft was observed in the TyrPC scaffolds after 16 weeks. A significant difference was observed between the lowest and highest doses, 10 and 50 μg of rhBMP-2, using radiographs ($p < 0.001$), 64-slice CT ($p < 0.001$), and micro-CT ($p < 0.003$). Histological analysis verified these findings and demonstrated organized bone formation into the defect. High correlation was observed between the different quantification methods used in this study, ranging between $R^2 = 0.446$ and 0.911 (Table 1). The correlation is also qualitatively evident from representative images of a sample from the 25 μg rhBMP-2 dose shown in Figure 6 (coronal cross-sectional images, Fig. 6A C; axial cross-sectional images Fig. 6D, E; and 3D renderings, Fig. 6F, G). Additionally, a comparison of the histological slices to corresponding 2D micro-CT sections showed a relatively higher correlation of $R^2 = 0.81$ compared with a correlation of $R^2 = 0.656$ between the histomorphometry and 3D micro-CT. It was observed that the correlation between the 2D slices and corresponding 3D values from the micro-CT data was even higher ($R^2 = 0.866$), indicating that the lower correlation between the histology and micro-CT data was only partially due to the modalities being compared across dimensions. Based on the correlation between methods reported in Table 1, the suggested sample size for each technique was calculated. Analysis of the suggested sample size to ensure detection of rhBMP-2 dose response (significant difference between 10 and 50 μg doses) showed that a total of six to eight rabbits/group was required to achieve a test with a power of 0.9 while keeping the probability of type I error < 0.05 (Table 2) while using radiographic techniques. When using histomorphometry, however, the suggested sample size to achieve the same significance between different doses of rhBMP-2 was 25 (Table 2).

Table 1. Correlation Between Analysis Techniques to Measure Bone Regenerated Within Defect Volume Using Pearson Correlation Statistics After Fisher's Z Transformation

	Histology	*Micro-CT*	*64-Slice CT*	*Radiography*
Radiography	0.446	0.798	0.759	1.000
64-Slice CT	0.749	0.911	1.000	0.759
Micro-CT	0.656	1.000	0.911	0.798
Histology	1.000	0.656	0.749	0.446

All correlations were significant at $p < 0.005$.
CT, computed tomography.

Discussion

Multiple techniques ranging from radiography to CT and histology were used to evaluate bone regeneration in the current study and it was found that the E1001(1k)+CP scaffold evaluated showed increased bone regeneration with increasing rhBMP-2 dose and time. Effective healing of the critical-size defect was observed at a fraction of the recommended dose (290 90 μg).[3–5] It is critical to use the minimal necessary dose of rhBMP-2 to regenerate bone so as to avoid possible complications such as imbalance in bone remodeling[8] or possible heterotopic ossification.[9] The maximum dose used in the current study was 50 μg, which is only 17% of the dose previously recommended by Smith *et al.* (430 μg/mL = 228 μg per defect)[5] and a fraction of that recommended for use with INFUSE (200 400 μg/mL = 106 212 μg per defect with a collagen sponge carrier) by Medtronics[27] for bone healing in rabbits. Even the 25 μg rhBMP-2 dose used showed significantly greater regenerated bone volume fraction than the control and 10 μg rhBMP-2 dose using the 64-slice CT.

It was also observed from the 64-slice CT analysis that between 4 and 16 weeks, the presence or absence of rhBMP-2 had a profound effect on bone regeneration. While the control group without rhBMP-2 increased by 65% from week 4 to 16 in terms of bone volume, the groups with rhBMP-2 increased by an average of 121% with no significant difference between various dosages of the growth factor. Similarly, the quality of the bone regenerated, measured by the mineral density of the bone within the defect space, also increased 27% without rhBMP-2 delivery, but

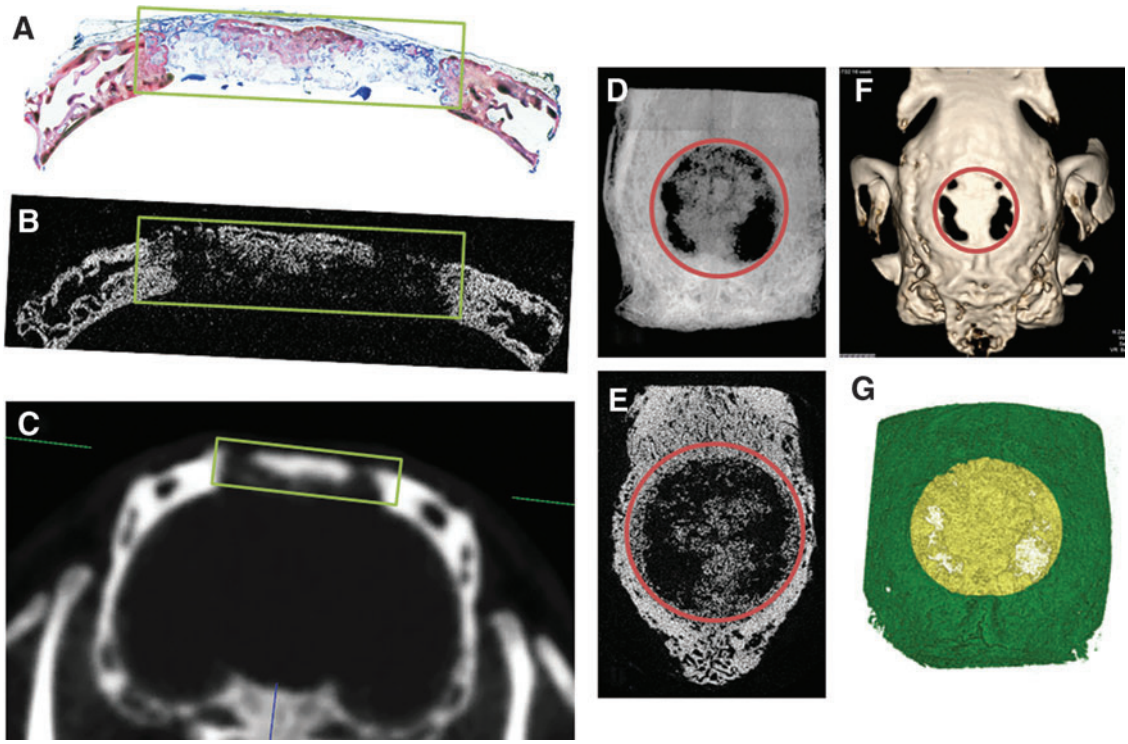

FIG. 6. A representative sample from the 25 μg rhBMP-2 dose group is chosen to highlight the qualitative visual similarity in results across evaluation techniques. Coronal sections through the defect center are shown using **(A)** histology, **(B)** micro-CT, and **(C)** clinical 64-slice CT after 16 weeks of implantation. Rectangles outline general defect area. **(D)** Coronal image using radiography, **(E)** a micro-CT coronal cross-section and 3D rendering using the **(F)** 64-slice CT, and **(G)** micro-CT data sets are also shown. Circles outline defect region. Color images available online at www.liebertpub.com/tec

increased by an average of 65% from week 4 to 16 when rhBMP-2 was delivered. While the presence of rhBMP-2 alone affected both bone quantity and quality in this study, across techniques radiography (50 μg > all other doses), 64-slice CT (50 μg > 25 μg > 10 μg, 0 μg), micro-CT (50 μg > 10 μg, 0 μg), and histology (50 μg, 25 μg > 0 μg) it was observed that in terms of total bone quantity regenerated, 10 μg was insufficient to observe noticeable differences from unloaded controls, 25 μg of rhBMP-2 resulted in greater bone volume regenerated, and 50 μg dose resulted in significantly greater quantities at 16 weeks.

A previous study by Hedberg *et al.*[1] compared the use of radiography, micro-CT, and histology to evaluate bone regeneration in a 15 mm defect in the rabbit radius. Their study was largely semiquantitative and dependent on scoring of bone regeneration, which introduces possible evaluator disparity and results in weaker statistical tests. Since then, the methods available for extensive quantification of bone regeneration in absolute terms have become widely available and are used in the current study resulting in far greater statistical confidence (Table 2). Hedberg *et al.*[1] also used radiography for longitudinal analysis of the defect site. While the approach was feasible and allowed for reproducibility and ease of access in their study since the radius can be imaged without interference from significant underlying ossified tissue, such is not the case with defects in the parietal bone of the calvaria. In this study, to overcome the limitations of radiography, we used 64-slice CT to evaluate the temporal sequence of bone healing by performing 3D analysis of live scans at 4 weeks and then at 16 weeks. The primary benefit of this approach is the ability to reduce the total number of animals used as the same animals were

Table 2. Relative Sample Sizes Required Based on Technique to Detect Significant Differences Between the rhBMP-2 Doses of 10 and 50 μg at 16 Weeks

	Radiography	*64-Slice CT*	*Micro-CT*	*Histology*
Difference between means	0.369	0.331	0.126	0.073
Residual standard deviation	0.161	0.132	0.062	0.067
Number of groups	4	4	4	4
Desired power of test	0.9	0.9	0.9	0.9
Alpha (α)	0.05	0.05	0.05	0.05
Sample size required	7	6	8	25

rhBMP 2, recombinant human bone morphogenetic protein 2.

Table 3. Relative Advantages and Drawbacks of Different Evaluation Techniques to Quantify Bone Regeneration in Preclinical Models

	Advantages	*Drawbacks*
Radiography	Non-destructive Fast and easy to perform Clinical availability Possible serial application (depending on anatomical site)	Two-dimensional visualization No depth perception Detects radio-opaque materials only Possible issues based on anatomical location
64-Slice CT	Non-destructive Available for clinical translation Relatively fast 3D visualization Can be repeated over course of healing for temporal trends Volume & density quantification	Low resolution vs. micro-CT Live scans require anesthesia No 3D morphological analysis for small-animal models Potential risk of X-ray exposure with frequent scans
Micro-CT	Non-destructive Fully quantitative for validation of all other techniques High spatial resolution at higher X-ray doses Three-dimensional morphometric analysis possible Vascularization visualization using enhanced contrast	Detects radio-opaque materials only High X-ray exposure if live Large quantities of digital data Time-consuming advanced analysis for quantification (less so than histology) Resolution still limited ~ 1 5 μm
Histology	Allows analysis of biological milieu Allows visualization of radiolucent scaffold materials Allows 2D histomorphometry Immunostaining for tissue-specific markers possible Cellular level resolution possible	Destructive Only serial 2D sections possible, high variability Highly labor intensive, time consuming, & operator sensitive Information depends on sectioning plane chosen

micro CT, micro computed tomography; 2D, two dimensional; 3D, three dimensional.

imaged at multiple time points with the associated effect of greater statistical confidence due to paired testing. The added advantage is that this technique is already available and widely used to evaluate bone healing clinically and in our study it shows high correlation to the far more sensitive and high-exposure micro-CT evaluation. Previous studies have used live clinical CT scans to evaluate bone regeneration patterns over an *in vivo* time course.[5,28] However, these studies were carried out at 1.5 mm resolution compared to the mean calvarial thickness of the rabbit being <3.5 mm in the parietal bone. In the current study, the 64-slice CT live scans were performed with a slice thickness of 0.5 mm and the data were upsampled using trilinear interpolation to a 20 μm resolution. While this does not allow for the calculation of 3D morphometric parameters, it allows for greater confidence in the determination of bone volume fraction and bone mineral density. In the case of larger animal models and in clinical settings, this method should also be able to estimate 3D histomorphometric parameters nondestructively. While it is possible to use *in vivo* live-animal micro-CT for monitoring of bone healing over time,[24] such methods come with associated risk of high radiation exposure and much longer scan times and may be limited by the size of the animal and the location of the defect being studied. In the current study, three rabbits were scanned simultaneously (in one full-length scan) on the bed of a clinical 64-slice CT scanner as opposed to individual longer scans using micro-CT. Correlation data demonstrate that the loss of resolution is acceptable in terms of recognizing bone regeneration patterns when considering the reduction in radiation dose and the potential clinical translation of the technique.

The advantages of using high-resolution micro-CT in terms of 3D morphometric parameter evaluation beyond simple bone volume fraction have been previously reported.[29] In the current study we used trabecular number (increase shows greater number of trabeculae) and Tb.Pf (decrease indicates an increase in connectivity[30]) to demonstrate that when the dose increased from 10 to 50 μg, the connectivity of the bony trabeculae formed increased significantly, indicating the bridging and functionality of the regenerated bone. The plots of spatial patterns of bone regenerated seemed to indicate a superior bias within the defect site, especially with the release of rhBMP-2. This could potentially stem from the fact that osteoprogenitors from the soft tissues covering the superior aspect of the defect responded more strongly to the released growth factor compared with those from the dural interface. Such observations could be further investigated in successive studies and might provide an indication of the most suitable source for deliverable stem cells to further accelerate defect healing.

Each analytical technique used in the current study provided a unique perspective in characterizing the nature of bone regeneration within the calvarial defects and the effects of rhBMP-2 dose. The relative advantages and drawbacks of each technique are summarized in Table 3. Radiography analysis provided quantifiable % defect coverage and radio-opacity, micro-CT provided spatial volumetric and bone density measures, histomorphometry provided biological confirmation of normal healing, and 64-slice CT allowed for time course analysis and establishing translational guidelines. To the best of our knowledge this is one of the first studies in which all four techniques have

been used and validated against one another. The statistical analysis based on the data generated in this study also allowed for confirmation that a sample size of six to eight animals per group is sufficient to distinguish difference in bone regeneration pattern between doses as close as 10 and 50 μg of rhBMP-2 over a 16-week study *in vivo* when radiographic techniques are used. Histological calculations showed the sample size required is much larger (25 samples/group), indicating either the sensitivity of the technique to dose effects was lower or the inconsistencies in basing the outcome on single slices introduced significant variance within groups. The latter rationale is supported because within group variance was highest for the histomorphometry measurements compared to the other techniques. Application of all these varied methodologies in conjunction with one another allowed for a standardized and comprehensive description of bone regeneration with significant clinical translational implications. In the future, with advances in resolution, it may also be possible to use additional techniques, such as magnetic resonance imaging[31] or contrast-enhanced CT,[32,33] to nondestructively image sequential monitoring of angiogenesis to provide further insight into the dynamics of *in vivo* bone regeneration.

Conclusions

A dose and temporal response of bone regeneration was observed to rhBMP-2 delivered from E1001(1k)+CP scaffolds in a critical-size rabbit calvarial defect. It was identified in this study that a 50 μg dose of rhBMP-2 regenerated significantly greater bone compared with a 10 μg dose. Radiography, 64-slice CT, micro-CT, and histological analyses were used in conjunction with one another to provide a comprehensive description of the quality, quantity, sequence, and biological nature of bone regenerated in the defect over 16 weeks of implantation. This allowed for a comparison between techniques and an assessment of their relative efficacy to assess dose responses to growth factors in a critical-sized defect model.

Acknowledgments

This research was sponsored in part by the Armed Forces Institute of Regenerative Medicine (AFIRM) award number W81XWH-08-2-0034 for which the U.S. Army Medical Research Acquisition Activity, 820 Chandler St., Fort Detrick, MD 21702-5014, is the awarding and administering acquisition office. This research was also supported in part by the U.S. Army of Surgical Research. T.G. would like to acknowledge support from USMRAA Grant number W81XWH-13-P-0075. The authors would like to acknowledge the assistance of Dr. Amit Vasanji, ImageIQ, with the 64-slice CT data analysis, and the assistance of Mr. Sean McBride, Dr. Jinku Kim, and Dr. Jeffry Hollinger, Carnegie Mellon University, with the preparation of the histological slides. The kind permission and support of the USAF Dental Evaluation and Consultation Service (DECS), Ft. Sam Houston, TX, Joint Base San Antonio for the use of the Skyscan 1072 micro-CT scanner and the Olympus microscope is also gratefully acknowledged. This study was conducted in compliance with the Animal Welfare Act and the Implementing Animal Welfare Regulations and in accordance with the principles of the Guide for the Care and Use of Laboratory Animals. All animal procedures were approved by the U.S. Army Institute of Surgical Research Animal Care and Use Committee. The opinions or assertions contained herein are the private views of the authors and are not to be construed as official positions or as reflecting the views of the Department of the Army or the Department of Defense.

Disclosure Statement

No competing financial interests exist.

References

1. Hedberg, E.L., Kroese Deutman, H.C., Shih, C.K., Le moine, J.J., Liebschner, M.A., Miller, M.J., *et al.* Methods: a comparative analysis of radiography, microcomputed tomography, and histology for bone tissue engineering. Tissue Eng **11,** 1356, 2005.
2. Edwards, P.C., Ruggiero, S., Fantasia, J., Burakoff, R., Moorji, S.M., Paric, E., *et al.* Sonic hedgehog gene enhanced tissue engineering for bone regeneration. Gene Ther **12,** 75, 2005.
3. Hou, R., Chen, F., Yang, Y., Cheng, X., Gao, Z., Yang, H.O., *et al.* Comparative study between coral mesenchymal stem cells rhbmp 2 composite and auto bone graft in rabbit critical sized cranial defect model. J Biomed Mater Res Part A **80A,** 85, 2007.
4. Rodgers, J.B., Vasconez, H.C., Wells, M.D., DeLuca, P.P., Faugere, M.C., Fink, B.F., *et al.* Two lyophilized polymer matrix recombinant human bone morphogenetic protein 2 carriers in rabbit calvarial defects. J Craniofac Surg **9,** 147, 1998.
5. Smith, D.M., Afifi, A.M., Cooper, G.M., Mooney, M.P., Marra, K.G., and Losee, J.E. Bmp 2 based repair of large scale calvarial defects in an experimental model: regener ative surgery in cranioplasty. J Craniofac Surg **19,** 1315, 2008.
6. McKay, W.F., Peckham, S.M., and Badura, J.M. A com prehensive clinical review of recombinant human bone morphogenetic protein 2 (infuse bone graft). Int Orthop **31,** 729, 2007.
7. Perri, B., Cooper, M., Lauryssen, C., and Anand, N. Ad verse swelling associated with use of rh bmp 2 in anterior cervical discectomy and fusion: a case study. Spine J **7,** 235, 2007.
8. Zara, J.N., Siu, R.K., Zhang, X., Shen, J., Ngo, R., Lee, M., *et al.* High doses of bone morphogenetic protein 2 induce structurally abnormal bone and inflammation *in vivo*. Tis sue Eng Part A **17,** 1389, 2011.
9. Axelrad, T.W., Steen, B., Lowenberg, D.W., Creevy, W.R., and Einhorn, T.A. Heterotopic ossification after the use of commercially available recombinant human bone mor phogenetic proteins in four patients. J Bone Joint Surg Br **90,** 1617, 2008.
10. Brown, K.V., Li, B., Guda, T., Perrien, D.S., Guelcher, S.A., and Wenke, J.C. Improving bone formation in a rat femur segmental defect by controlling bone morphogenetic protein 2 release. Tissue Eng Part A **17,** 1735, 2011.
11. Kolambkar, Y.M., Boerckel, J.D., Dupont, K.M., Bajin, M., Huebsch, N., Mooney, D.J., *et al.* Spatiotemporal delivery of bone morphogenetic protein enhances functional repair of segmental bone defects. Bone **49,** 485, 2011.
12. Schmitz, J.P., and Hollinger, J.O. The critical size defect as an experimental model for craniomandibulofacial non unions. Clin Orthop Relat Res **205,** 299, 1986.

13. An, Y.H., and Friedman, R.J. Animal models of bone de fect repair. In: An, Y.H., and Friedman, R.J. (eds.) Animal Models in Orthopaedic Research. Boca Raton, FL: Taylor & Francis Group, LLC, 1999, pp. 241 260.
14. Aaboe, M., Pinholt, E.M., Schou, S., and Hjorting Hansen, E. Incomplete bone regeneration of rabbit calvarial defects using different membranes. Clin Oral Implants Res **9,** 313, 1998.
15. Chen, T. M., Yao, C. H., Wang, H. J., Chou, G. H., Lee, T. W., and Lin, F. H. Evaluation of a novel malleable, biodegradable osteoconductive composite in a rabbit cra nial defect model. Mater Chem Phys **55,** 44, 1998.
16. Dean, D., Topham, N.S., Meneghetti, S.C., Wolfe, M.S., Jepsen, K., He, S., *et al.* Poly(propylene fumarate) and poly(dl lactic co glycolic acid) as scaffold materials for solid and foam coated composite tissue engineered con structs for cranial reconstruction. Tissue Eng **9,** 495, 2003.
17. Hammerle, C.H., Schmid, J., Lang, N.P., and Olah, A.J. Temporal dynamics of healing in rabbit cranial defects using guided bone regeneration. J Oral Maxillofac Surg **53,** 167, 1995.
18. Lam, C.X., Hutmacher, D.W., Schantz, J.T., Woodruff, M.A., and Teoh, S.H. Evaluation of polycaprolactone scaffold degradation for 6 months *in vitro* and *in vivo*. J Biomed Mater Res A **90,** 906, 2009.
19. Levy, F.E., Hollinger, J.O., and Szachowicz, E.H. Effect of a bioresorbable film on regeneration of cranial bone. Plast Reconstr Surg **93,** 307, 1994; discussion 312.
20. Yao, C.H., Liu, B.S., Hsu, S.H., and Chen, Y.S. Calvarial bone response to a tricalcium phosphate genipin cross linked gelatin composite. Biomaterials **26,** 3065, 2005.
21. Magno, M.H.R., Kim, J., Srinivasan, A., McBride, S., Bolikal, D., Darr, A., *et al.* Synthesis, degradation and biocompatibility of tyrosine derived polycarbonate scaf folds. J Mater Chem **20,** 8885, 2010.
22. Kim, J., Magno, M.H., Alvarez, P., Darr, A., Kohn, J., and Hollinger, J.O. Osteogenic differentiation of pre osteoblasts on biomimetic tyrosine derived polycarbonate scaffolds. Biomacromolecules **12,** 3520, 2011.
23. Kim, J., Magno, M.H., Waters, H., Doll, B.A., McBride, S., Alvarez, P., *et al.* Bone regeneration in a rabbit critical sized calvarial model using tyrosine derived polycarbonate scaffolds. Tissue Eng Part A **18,** 1132, 2012.
24. Bouxsein, M.L., Boyd, S.K., Christiansen, B.A., Guldberg, R.E., Jepsen, K.J., and Müller, R. Guidelines for assessment of bone microstructure in rodents using micro computed tomography. J Bone Miner Res **25,** 1468, 2010.
25. Otsu, N. A threshold selection method from gray level histograms. Automatica **11,** 23, 1975.
26. Dumas, J.E., BrownBaer, P.B., Prieto, E.M., Guda, T., Hale, R.G., Wenke, J.C., *et al.* Injectable reactive bio composites for bone healing in critical size rabbit calvarial defects. Biomed Mater **7,** 024112, 2012.
27. McKay, W.F., Peckham, S.M., and Marotta, J.S. The Sci ence of rhbmp 2. St. Louis, MO: Quality Medical Pub lishing, Inc., 2006.
28. Smith, D.M., Cooper, G.M., Afifi, A.M., Mooney, M.P., Cray, J., Rubin, J.P., *et al.* Regenerative surgery in cra nioplasty revisited: the role of adipose derived stem cells and bmp 2. Plast Reconstr Surg **128,** 1053, 2011.
29. Efeoglu, C., Fisher, S.E., Erturk, S., Oztop, F., Gunbay, S., and Sipahi, A. Quantitative morphometric evaluation of critical size experimental bone defects by microcomputed tomography. Br J Oral Maxillofac Surg **45,** 203, 2007.
30. Hahn, M., Vogel, M., Pompesius Kempa M, and Delling, G. Trabecular bone pattern factor a new parameter for simple quantification of bone microarchitecture. Bone **13,** 327, 1992.
31. Beaumont, M., DuVal, M.G., Loai, Y., Farhat, W.A., Sandor, G.K., and Cheng, H.L. Monitoring angiogenesis in soft tissue engineered constructs for calvarium bone re generation: an *in vivo* longitudinal DCE MRI study. NMR Biomed **23,** 48, 2010.
32. Arkudas, A., Beier, J.P., Pryymachuk, G., Hoereth, T., Bleiziffer, O., Polykandriotis, E., *et al.* Automatic quanti tative micro computed tomography evaluation of angio genesis in an axially vascularized tissue engineered bone construct. Tissue Eng Part C Methods **16,** 1503, 2010.
33. Young, S., Kretlow, J.D., Nguyen, C., Bashoura, A.G., Baggett, L.S., Jansen, J.A., *et al.* Microcomputed tomog raphy characterization of neovascularization in bone tissue engineering applications. Tissue Eng Part B Rev **14,** 295, 2008.

Address correspondence to:
Pamela R. Brown Baer, MEd, DDS
Department of Craniomaxillofacial Regenerative Medicine
Dental and Trauma Research Detachment
United States Army Institute of Surgical Research
3698 Chambers Pass
Fort Sam Houston, TX 78234

E-mail: pamela.r.brownbaer.civ@mail.mil

Received: September 16, 2013
Accepted: January 6, 2014
Online Publication Date: February 28, 2014